

NO-A182 709 EXTREME RUNUP STATISTICS ON NATURAL BEACHES(U) OFFSHORE 1/1
AND COASTAL TECHNOLOGIES INC VICKSBURG MS D T RESIO
MAY 87 CERC-MP-87-11 DACH39-85-M-4864

NO-A182 709 EXTREME RUNUP STATISTICS ON NATURAL BEACHES(U) OFFSHORE 1/1
AND COASTAL TECHNOLOGIES INC VICKSBURG MS D T RESIO
MAY 87 CERC-MP-87-11 DACH39-85-M-4864

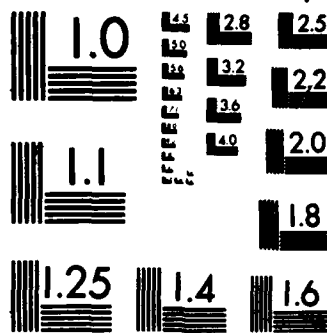
NO-A182 709 EXTREME RUNUP STATISTICS ON NATURAL BEACHES(U) OFFSHORE 1/1
AND COASTAL TECHNOLOGIES INC VICKSBURG MS D T RESIO
MAY 87 CERC-MP-87-11 DACH39-85-M-4864

UNCLASSIFIED F/G 8/3 NL

UNCLASSIFIED F/G 8/3 NL

UNCLASSIFIED F/G 8/3 NL

██████████	██████████	██████████	██████████	END
██████████	██████████	██████████	██████████	8-87
██████████	██████████	██████████	██████████	DTIC



MICROCOPY RESOLUTION TEST CHART
NATIONAL BUREAU OF STANDARDS-1963-A

DTIC FILE COPY

MISCELLANEOUS PAPER CERC-87-11

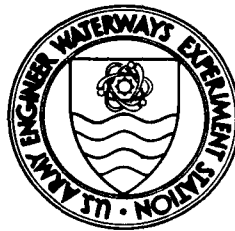
12

EXTREME RUNUP STATISTICS ON NATURAL BEACHES

by

Donald T. Resio

Offshore & Coastal Technologies, Inc.
911 Clay St.
Vicksburg, Mississippi 39180



May 1987

Final Report

Approved For Public Release; Distribution Unlimited

DTIC
ELECTE
JUL 16 1987
S D
E

Prepared for DEPARTMENT OF THE ARMY
US Army Corps of Engineers
Washington, DC 20314-1000

Monitored by Coastal Engineering Research Center
US Army Engineer Waterways Experiment Station
PO Box 631, Vicksburg, Mississippi 39180-0631

Under Contract No. DACW39-85-M-4064

87

ADA182709

REPORT DOCUMENTATION PAGE				Form Approved OMB No 0704-0188 Exp Date Jun 30, 1986	
1a. REPORT SECURITY CLASSIFICATION Unclassified			1b. RESTRICTIVE MARKINGS		
2a. SECURITY CLASSIFICATION AUTHORITY			3. DISTRIBUTION/AVAILABILITY OF REPORT Approved for public release; distribution unlimited		
2b. DECLASSIFICATION/DOWNGRADING SCHEDULE			5. MONITORING ORGANIZATION REPORT NUMBER(S) Miscellaneous Paper CERC-87-11		
4. PERFORMING ORGANIZATION REPORT NUMBER(S)			7a. NAME OF MONITORING ORGANIZATION USAEWES, Coastal Engineering Research Center		
6a. NAME OF PERFORMING ORGANIZATION Offshore & Coastal Technologies, Inc.		6b. OFFICE SYMBOL (if applicable)		7b. ADDRESS (City, State, and ZIP Code) PO Box 631 Vicksburg, MS 39180-0631	
6c. ADDRESS (City, State, and ZIP Code) 911 Clay St. Vicksburg, MS 39180		8b. OFFICE SYMBOL (if applicable)		9. PROCUREMENT INSTRUMENT IDENTIFICATION NUMBER DACW39-85-M-4064	
8a. NAME OF FUNDING/SPONSORING ORGANIZATION US Army Corps of Engineers		8c. ADDRESS (City, State, and ZIP Code) Washington, DC 20314-1000		10. SOURCE OF FUNDING NUMBERS	
				PROGRAM ELEMENT NO	PROJECT NO
				TASK NO	WORK UNIT ACCESSION NO
11. TITLE (Include Security Classification) Extreme Runup Statistics on Natural Beaches					
12. PERSONAL AUTHOR(S) Resio, Donald T.					
13a. TYPE OF REPORT Final report		13b. TIME COVERED FROM _____ TO _____		14. DATE OF REPORT (Year, Month, Day) May 1987	
				15. PAGE COUNT 29	
16. SUPPLEMENTARY NOTATION Available from National Technical Information Service, 5285 Port Royal Road, Springfield, VA 22161.					
17. COSATI CODES			18. SUBJECT TERMS (Continue on reverse if necessary and identify by block number)		
FIELD	GROUP	SUB-GROUP	Expected extreme runups		
			Natural beaches		
			Wave runup		
19. ABSTRACT (Continue on reverse if necessary and identify by block number)					
<p>Wave runup data collected on a natural beach at the Coastal Engineering Research Center's Field Research Facility (FRF) are analyzed. The FRF data are supplemented by additional runup data collected on two beaches within San Francisco Bay, California. Analyses focused on developing a method to predict the upper limit of wave runup on natural beaches.</p> <p>It was found that beach runup at the FRF was strongly dependent on a surf similarity parameter based on beach face slope and incident wave conditions. However, correlation between the runup and surf parameter was quite sensitive to the location where wave conditions were measured. Runup predictions using wave information from a gage in 8 m of water were better than similar predictions using information from gages in depths of 17 and 2 m. It was also found that scaling using the local wave length was superior to scaling by the deep-water wave length.</p>					
(Continued)					
20. DISTRIBUTION/AVAILABILITY OF ABSTRACT <input checked="" type="checkbox"/> UNCLASSIFIED/UNLIMITED <input type="checkbox"/> SAME AS RPT <input type="checkbox"/> DTIC USERS			21. ABSTRACT SECURITY CLASSIFICATION Unclassified		
22a. NAME OF RESPONSIBLE INDIVIDUAL			22b. TELEPHONE (Include Area Code)		22c. OFFICE SYMBOL

Unclassified

SECURITY CLASSIFICATION OF THIS PAGE

19. ABSTRACT (Continued).

A statistical framework is developed for estimating the extreme wave runup during a storm. This framework is specifically applicable to the FRF, but analysis indicates that it is general enough to be used for the San Francisco Bay beaches and possibly for most natural sand beaches. For idealized, constant conditions, a simple procedure is presented for estimating the expected maximum runup elevation during a storm. *Keywords:*

Beach erosion; ocean waves; oceanography

Unclassified

SECURITY CLASSIFICATION OF THIS PAGE

Preface

This report discusses analyses of wave runup data collected on natural sand beaches and presents a method to estimate maximum runup elevation on a beach during a storm. The work was sponsored through funds provided to the US Army Engineer Waterways Experiment Station (WES) by the Civil Works Directorate, Office, Chief of Engineers (OCE), US Army Corps of Engineers, under the Coastal Structures Evaluation and Design Program Work Unit entitled Wave Runup and Overtopping. The report was prepared under Contract No. DACW39-85-M-4064. OCE Technical Monitors for this research were Messrs. J. H. Lockhart and J. G. Housley.

Analyses were performed and the report written by Dr. Donald T. Resio of Offshore & Coastal Technologies, Inc. The effort was coordinated by Mr. John P. Ahrens, oceanographer, under the general supervision of Dr. James R. Houston, Chief of the Coastal Engineering Research Center; Mr. C. E. Chatham, Chief of the Wave Dynamics Division; and Mr. D. D. Davidson, Chief of the Wave Research Branch. This report was edited by Ms. J. W. Leach of the Information Technology Laboratory, WES.

Commander and Director of WES during publication of this report was COL Dwayne G. Lee, CE. Technical Director was Dr. Robert W. Whalin.

Accession For	
NTIS GRA&I	<input checked="checked" type="checkbox"/>
DTIC TAB	<input type="checkbox"/>
Unannounced	<input type="checkbox"/>
Justification	
By	
Distribution/	
Availability Codes	
Dist	Avail and/or Special
A-1	



Contents

	<u>Page</u>
Preface.....	1
List of Figures.....	3
Introduction.....	4
Basic Physics of Wave Transformations Related to Extreme Runup Prediction.....	4
Statistical Estimation of Runup Extremes.....	11
New Data Sets.....	16
Analysis of Available Data.....	18
Analysis of R_2 and \hat{R}_2	18
Analysis of $F(\hat{R})$	18
Conclusions and Recommendations.....	22
References.....	25
Tables 1 and 2	

List of Figures

<u>No.</u>		<u>Page</u>
1	Plot of \hat{R}_2 versus ξ	6
2	Results of analysis of Holman data set based on wave conditions at gage 620.....	8
3	Results of analysis of Holman data set based on wave conditions at gage 625.....	8
4	Results of analysis of Holman data set based on wave conditions at gage 615.....	9
5	Results of analysis of Holman data set based on wave conditions at gage 620 with the local wavelength used as the horizontal length-scale parameter.....	10
6	Results of analysis of Holman data set based on wave conditions at gage 625 with the local wavelength used as the horizontal length-scale parameter.....	10
7	Results of analysis of Holman data set based on wave conditions at gage 615 with the local wavelength used as the horizontal length-scale parameter.....	11
8	Schematic representation of the three Fisher-Tippett asymptotic distributions on X-Y diagrams.....	15
9	Maps showing locations of Alameda Beach and Coyote Point field sites.....	17
10	Data taken from the Carlson experiments plotted against the background of Figure 3, gage 625.....	19
11	Sample of 15 largest runups for 32 selected cases from Holman.....	20
12	Plot of extremal distribution for expected runups.....	22
13	Plot of Alameda Beach data from analysis of the Carlson data.....	23
14	Plot of Coyote Point data from analysis of the Carlson data.....	23

EXTREME RUNUP STATISTICS ON NATURAL BEACHES

Introduction

1. Although active research into the estimation of runup has been under way for many years, comprehensive guidance presently does not exist for the estimation of expected runup extremes on natural beaches. Holman (1986) used extensive data collected at the Coastal Engineering Research Center's (CERC) Field Research Facility (FRF) to formulate statistical relationships between input wave parameters and extreme runup parameters. However, his analysis did not address questions related to the selection of appropriate wave parameters, nor did it consider data from sites other than the FRF. The objective of this report will be to supplement FRF data with data from additional sites, to examine consistency of wave data taken from different depths relative to the prediction of runup, and to formulate a statistical framework for estimating extreme runups during a storm.

Basic Physics of Wave Transformations Related to Extreme Runup Prediction

2. The dynamics of waves approaching a coast, although very complex, have become better understood in the last few years. Much of this new understanding stems from the increased availability of high-quality wave measurements in shallow water. Bouws et al. (1985) compiled and analyzed an extensive data set which demonstrates that, even in shallow water, wave spectra during storm conditions appear to maintain a predictable spectral shape. Resio (1986a, 1986b) presented a theoretical argument which appears to explain some of the reasons for this strong tendency toward an equilibrium form.

3. A primary question which relates to prediction of runup on a natural beach (or on a structure, for that matter) is where should the wave information be obtained in order to achieve the best prediction of runup phenomena. Should it be taken from deep water, from outside the surf zone in shallow water, or from inside the surf zone? Should wave parameters consider local wave steepness or deep-water steepness? Holman (1986) does not address this question but, rather, seems to imply that it really does not make too much difference.

4. An examination of these questions begins by specifying relevant wave parameters and runup parameters involved in actual prediction of runup on a beach. If the analysis of Holman is followed, it can be seen that runup and incident wave conditions can be linked by an equation (Hunt's equation) of the form:

$$\frac{R}{H} = \frac{\tan \beta}{\sqrt{H/L}} \quad (1)$$

where

R = arbitrary runup parameter

H = arbitrary wave height parameter

β = beach slope angle (defined to be positive)

L = arbitrary wavelength parameter

Figure 1 from Holman's paper shows a plot of \hat{R}_2 versus ξ , where \hat{R}_2 is defined as

$$\hat{R}_2 = \frac{R_2}{H_{m_0}} \quad (2)$$

where

R_2 = runup only exceeded by 2 percent of all runups

H_{m_0} = zero-moment wave height

ξ is defined as

$$\xi = \frac{\tan \beta}{\sqrt{H_{m_0}/L_0}} \quad (3)$$

where L_0 = deep-water wavelength associated with spectral peak frequency;
i.e.

$$L_0 = \frac{g}{2\pi} T_m^2 \quad (4)$$

where

g = acceleration due to gravity

T_m = spectral peak period

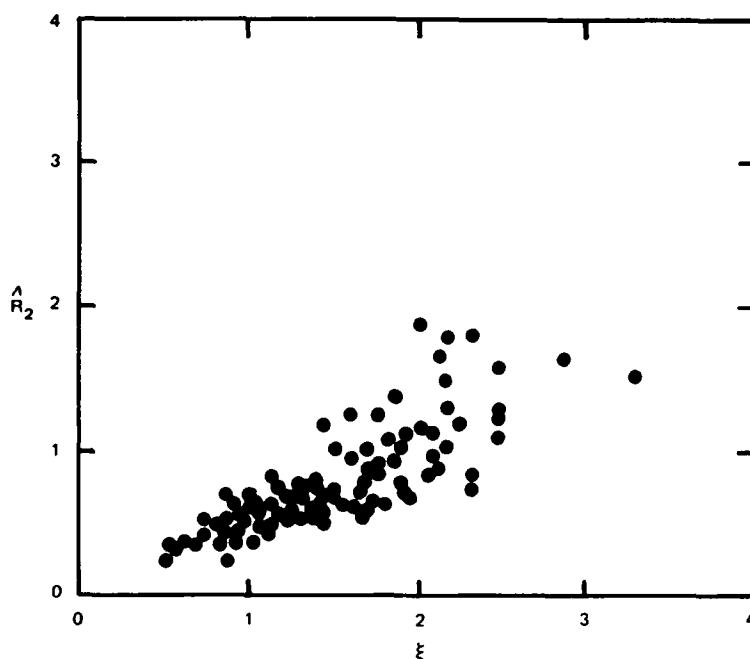


Figure 1. Plot of \hat{R}_2 versus ξ
(after Holman 1986)

In this figure, wave data represent wave heights and periods measured at gage 625, which is located at the seaward end of the pier in about 7 m of water. According to Holman, wave conditions at gage 625 are quite similar, at least in a statistical context, to those at gage 620, which is located farther offshore in about 17 m of water.

5. One might assume from Holman's presentation that the location of wave data is not very important to the accurate prediction of wave runup on natural beaches. Since wave height enters linearly on the left-hand side of Equation 1 and inside a square root on the right-hand side, it is only strictly possible for Holman's argument to hold if the wave height remains constant from gage 620 to gage 625. Thus, Holman's comment that the data are statistically similar suggests that, on the average, wave heights at gages 620 and 625 are fairly similar. Whereas this might on the average be true for waves at gages 620 and 625, it may not be true in general for waves measured at arbitrary locations (depths) from the shoreline. Also, it can be seen not to be true for certain specific instances, even for gages 620 and 625.

Table 1 lists wave heights and periods for two selected time intervals covered by Holman's data. During the first of these intervals, the waves are very long (peak periods in excess of 16 sec) and wave heights at gage 620 are only moderate (2.2 to 2.5 m). Therefore, the waves are not very steep (swell waves), and wave shoaling appears to add more energy into the waves than is removed by dissipative processes (nonlinear fluxes, wave breaking, bottom friction, etc.). By the time these waves arrive at gage 625, wave heights are in excess of 3 m. In the latter interval, wave periods are shorter (8.0 to 13.5 sec) and wave heights are large (~4 m) and very steep (storm waves). In this case, dissipative processes remove more energy from the spectrum than is added by shoaling, resulting in lower wave heights at gage 625. From examination of these two separate events, it seems that the wave transformation process between gages 620 and 625 is sensitive to wave steepness. This is consistent with the nonlinear flux theory advanced by Resio (1986a, 1986b).

6. In an effort at least to initiate some examination of the applicability of various wave parameters from different offshore locations for use in wave runup predictions, the following analyses were performed. First, an attempt was made to isolate only those spectra believed likely to have one dominant spectral peak. Since it is obvious that one peak period cannot provide a realistic predictive parameter for multimodal spectra, this step should remove some extraneous scatter from Holman's plots of \hat{R}_2 versus ξ . Having examined a wide range of spectra from the FRF site over the years, it was observed that most strongly multimodal spectra were associated with low seas; therefore, as a first stratification level, all cases for which the wave height at gage 620 was under 1 m were excluded. As a second level of stratification, all cases in which the peak period changed by over 1.5 sec between gages 620 and 625 were removed. After this processing was complete, computer plots were generated of \hat{R}_2 versus ξ , in which deep-water wavelength was used as the horizontal length parameter. Figures 2-4 show results of the analysis of the Holman data set based on wave conditions at gages 620, 625, and 615, respectively. Plots for 620 and 625 are similar, in agreement with Holman's conclusions. However, the plot based on data from gage 615 shows little agreement with the others, nor is much of a general pattern in the relationship between \hat{R}_2 and ξ evident in the analysis based on gage 615. This suggests that data inside or very near the surf zone are probably not good predictors of runup.

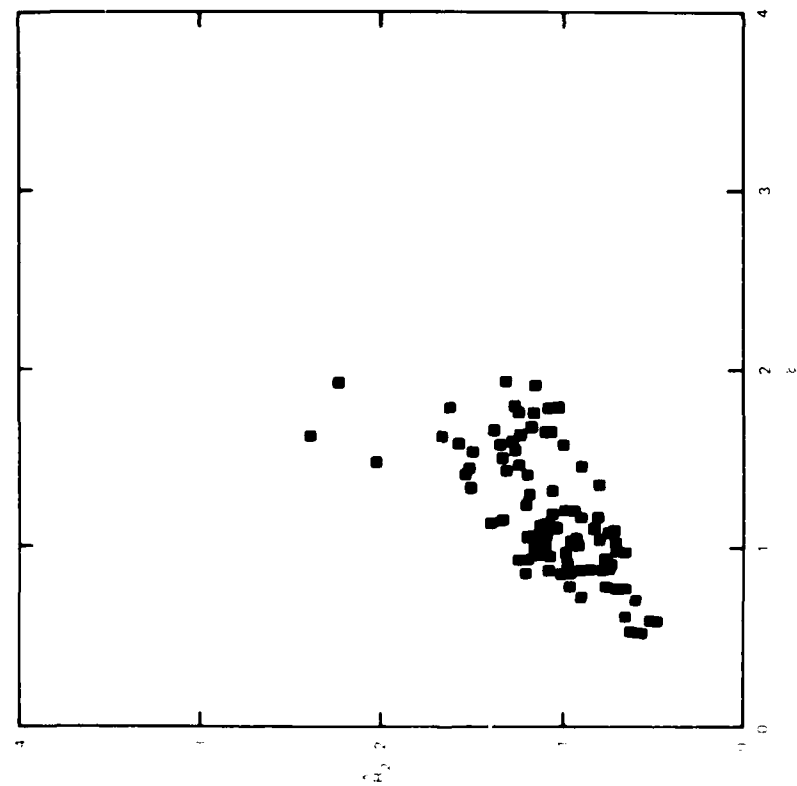


Figure 2. Results of analysis of Holman data set
based on wave conditions at gage 620

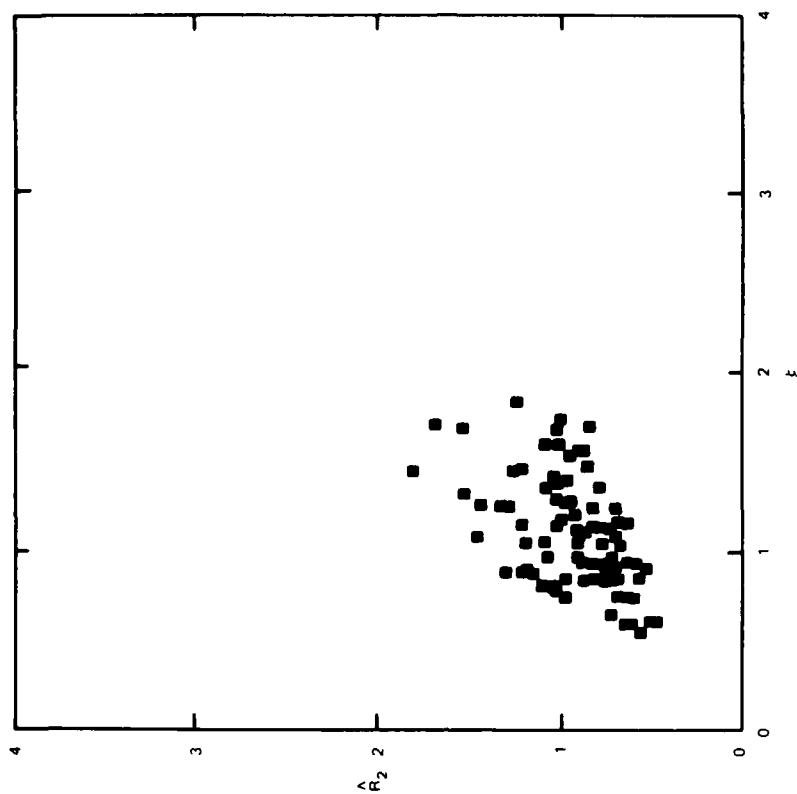


Figure 3. Results of analysis of Holman data set
based on wave conditions at gage 625

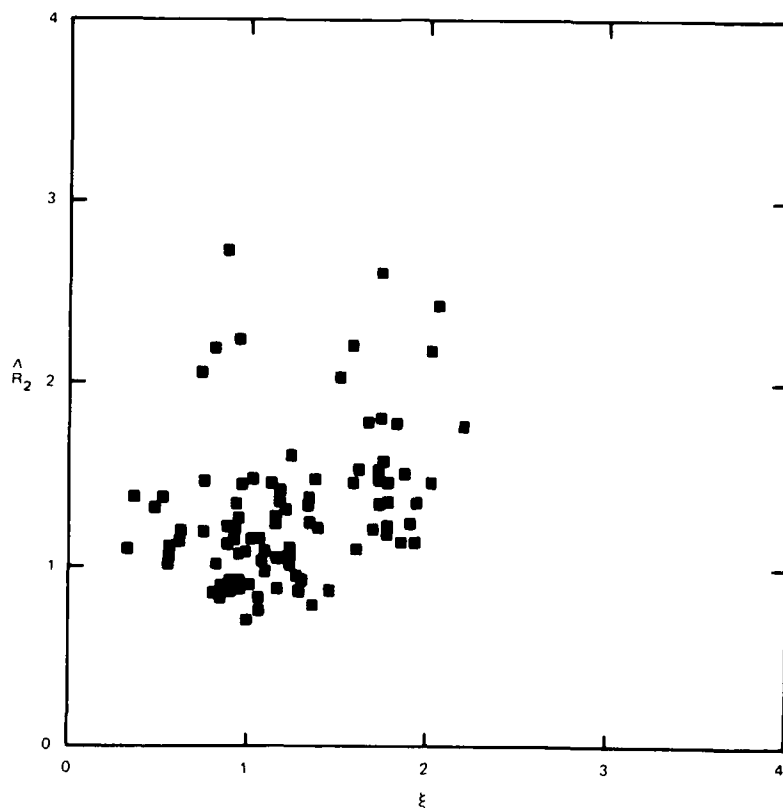


Figure 4. Results of analysis of Holman data set based on wave conditions at gage 615

7. One possible explanation of lack of agreement between runup data and wave parameters at gage 615 lies in the very shallow depth at that site (about 1.5 m average depth). Tidal variations and local deposition and erosion produce large variations in total depth. This variation is much larger percentagewise than variations at gages 620 and 625.

8. Figures 5-7 show plots similar to Figures 2-4; however, this time the local wavelength has been used as the horizontal length-scale parameter. Comparisons between gages indicate that use of the local length scale appears to significantly reduce scatter in the relationship between \hat{R}_2 and ξ for all three gages.

9. One aspect of the plots based on local wavelength scaling is that three points appear as outliers for the plot based on the gage 620 data (Figure 5), whereas these same three points do not appear as outliers in the plot based on the gage 625 data. The same three outliers also can be seen in the plot based on gage 620 using deep-water wavelength scaling. All three of these points come from measurements at 1700 on 14 October. At that time the

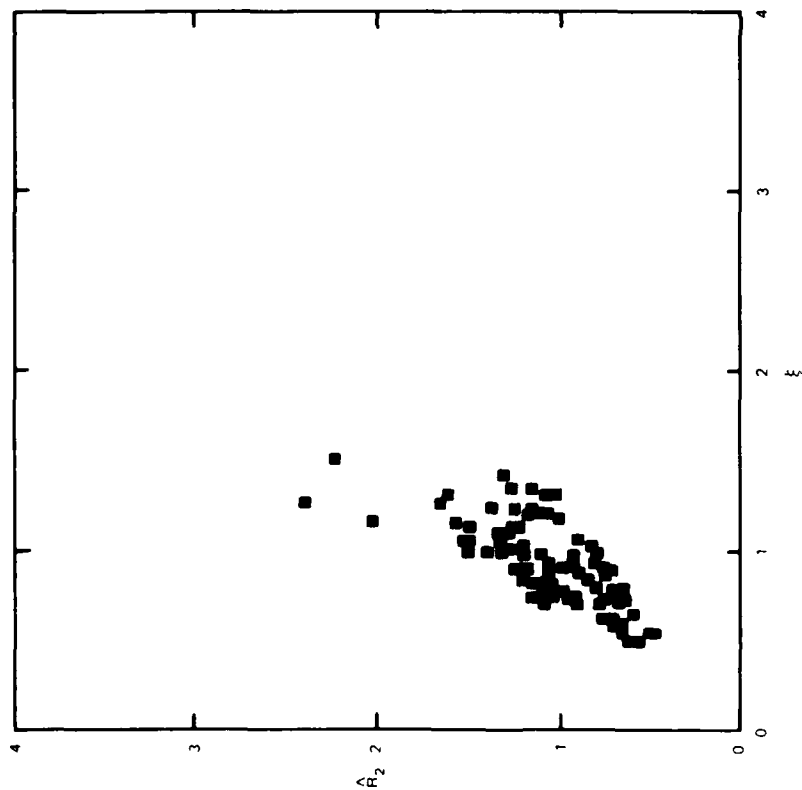


Figure 5. Results of analysis of Holman data set based on wave conditions at gage 620 with the local wavelength used as the horizontal length-scale parameter

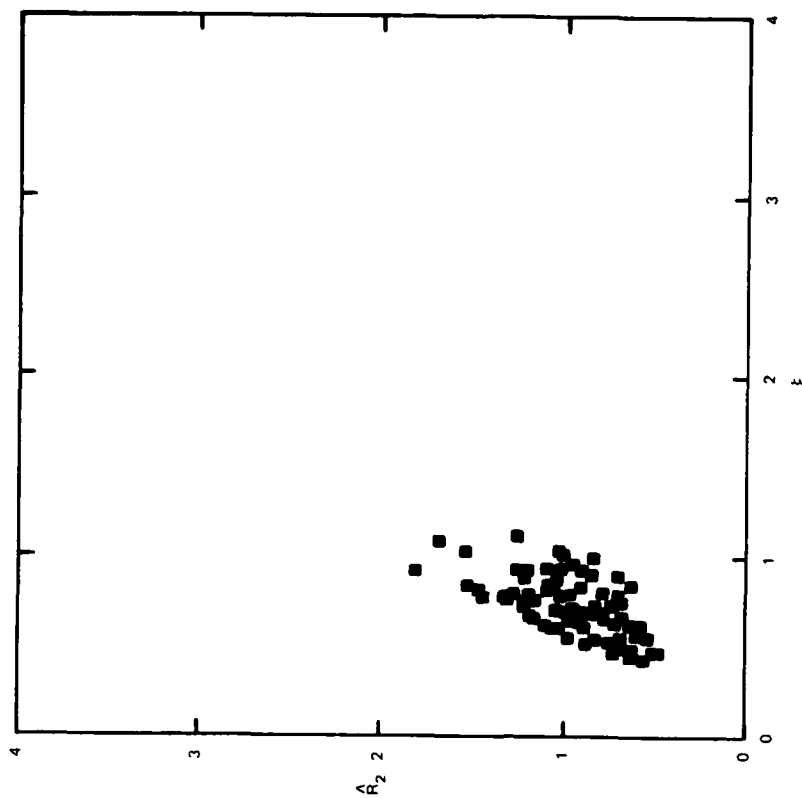


Figure 6. Results of analysis of Holman data set based on wave conditions at gage 625 with the local wavelength used as the horizontal length-scale parameter

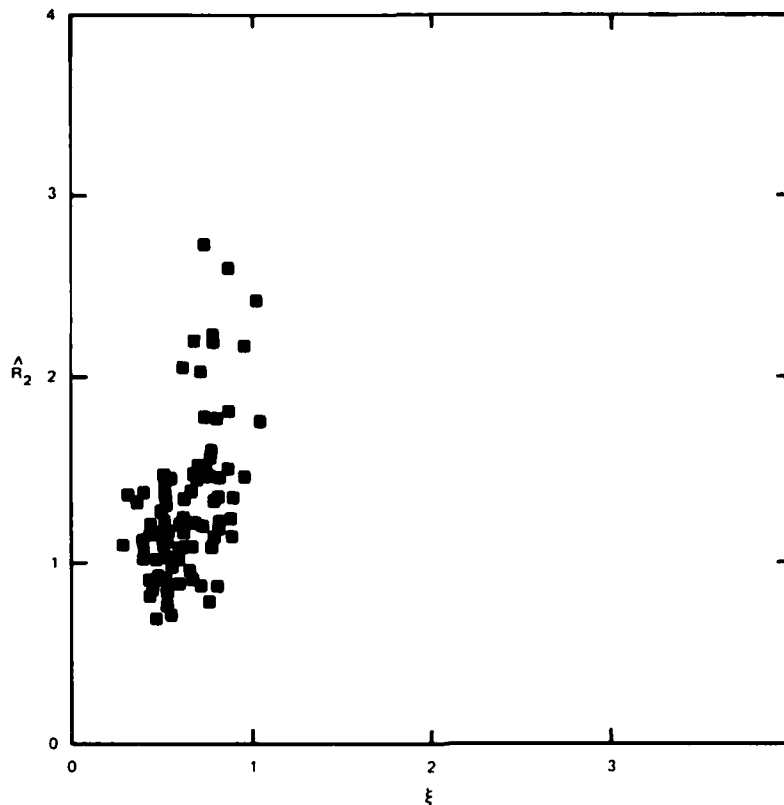


Figure 7. Results of analysis of Holman data set based on wave conditions at gage 615 with the local wavelength used as the horizontal length-scale parameter

wave height at gage 620 was only 1.11 m and shoaled to a 1.47-m value at gage 625. This increase in wave height at gage 625 reduces the value of \hat{R}_2 , and the increase in wave height plus the reduction in wave length at gage 625 combines to increase the value of ξ at gage 625. These combined effects bring these outliers more into line with the general pattern between \hat{R}_2 and ξ . Thus, it appears that waves at gage 625 using local wavelength scaling provide the most consistent predictor of runup.

Statistical Estimation of Runup Extremes

10. Each individual runup is related to incident wave parameters such as H_{m0} and T_m in a probabilistic fashion. Consequently, the relationship between distribution of individual runups and incident wave parameters can be written in a conditional probability statement much in the same way as the

relationship between individual wave heights and statistical wave parameters (such as mean wave height and significant wave height). Most of the analyzed records cover only a time interval of about 20 min; consequently, maximum runup is typically only about the same magnitude of the 1-percent wave height for wave periods around 12 sec. This estimated runup cannot be regarded as the maximum runup expected over an entire storm, which typically will have a duration of 6 to 48 hr. Since the expected largest single runup during a storm can be an important design consideration in locating and designing certain structures in coastal environments, a methodology will be developed here to provide the framework for a reasonable estimate of this parameter.

11. Over the course of a single storm, storm surge, wave setup, and astronomical tide all can contribute to time-varying changes in location of the base level for the runup process. Also, incident wave heights, wave periods, wave directions, and possibly beach slope vary throughout the storm. Since all these factors enter into estimation of runup elevations, it is not always clear, a priori, which conditions will produce the maximum potential for runup. One could introduce arbitrary factors and conservatism into runup estimates by attempting to select a constant set of wave, water-level, and beach parameters for a fixed duration supposedly equivalent to the expected runup produced by actual time-histories of the processes. However, it is possible to derive a more precise estimate by an appropriate convolution integral over the entire storm.

12. As stated previously, for a set of fixed conditions, the cumulative frequency distribution F of individual runups can be written in terms of a conditional probability, i.e.

$$F_t(R_1) = F_t(R_1 | \underline{\epsilon}) p(\underline{\epsilon}) \quad (5)$$

where

$\underline{\epsilon}$ = a vector consisting of all parameters influencing the statistical properties of runup

p = probability density function

t = estimate for conditions at a particular time

For a reasonably complete set of these parameters one might take

$$\underline{\varepsilon} = \left(H_{m_0}, T_m, \bar{\theta}, \eta, \beta \right) \quad (6)$$

where

$\bar{\theta}$ = mean wave direction at the location where H_{m_0} and T_m are obtained

η = mean water level (MWL) (MWL + tide + surge + setup)

If a nonexceedance probability $P_t(R_i)$ is defined as

$$P_t(R_i) = 1 - F_t(R_i) \quad (7)$$

then over two time intervals with approximately constant conditions within each (but possibly with differences in $\underline{\varepsilon}$ between the two times) one has

$$P_{t_1} \times t_2(R_i) = P_{t_1}(R_i) \times P_{t_2}(R_i) \quad (8)$$

or in general over any arbitrary number of time increments one has

$$P_e(R_i) = \prod_{k=1}^n P_{t_k}(R_i) \quad (9)$$

where the subscript e denotes that the nonexceedance probability is for an entire event.

13. Following the procedure derived by Borgman (1973) for maximum wave heights, one can now write an integral for the expected largest runoff over the entire storm as

$$F_e(R_i) = 1 - \exp \left\{ \int_0^t \ln [P_t(R_i)] \frac{dt}{\bar{T}} \right\} \quad (10)$$

where \bar{T} = mean period of runups. Equation 10 can be used in a discretized form in a numerical integration scheme over a storm, i.e.

$$F_e(R_1) = 1 - \exp \left\{ \sum_{k=1}^n \ln \left[1 - F_{t_k}(R_1) \right] \frac{\Delta t_k}{\bar{T}_k} \right\} \quad (11)$$

where $\Delta t_k / \bar{T}_k$ = number of runups in the k^{th} time increment. Equation 11 provides a convenient form to incorporate as many of the parameters in Equation 5 as desired into the estimation of expected largest runup over the storm. Also, in a rather straightforward application, the methodology described here can be used in a general way to estimate the largest n runups (i.e. largest two runups, three runups, etc.), which might also influence design and planning considerations.

14. Viewing Equation 11, it becomes evident that accurate estimation of the cumulative distribution function is of central importance to determination of extreme runups. Some past methodologies have fit the entire runup distribution to certain theoretical forms such as the Weibull distribution. Whereas this is a good technique for characterization of general runup patterns, it does not necessarily ensure a good fit to the "tail" of the distribution which controls extreme runups. Consequently, it is recommended that asymptotic methods be used. In particular, the so-called generalized extreme value (GEV) method is seen as capable of providing good estimates of expected sample extremes.

15. It has been shown (Fisher and Tippett 1928) that if one excludes certain improper distributions, there are only three asymptotic limiting forms for extremal distributions. These are given by

$$\begin{array}{lll} \text{I} & \phi(x) = \exp [-\exp (-x)] & \text{for } -\infty < x \leq \infty \\ \text{II} & \phi(x) = \exp [-(c/x)^{k'}] & \text{for } x \geq 0 \\ & = 0 & \text{for } x < 0 \\ \text{III} & \phi(x) = 1 & \text{for } x \geq w \\ & = \exp [-c(w-x)^{k'}] & \text{for } x < w \end{array}$$

where

x = generalized variant

c, k', w = parameters of asymptotic extreme-value distributors in original forms due to Fisher and Tippett (1928)

Jenkinson (1955) showed that all three asymptotic distributions could be written in a common form

$$x = x_0 + \alpha \left(\frac{1 - e^{-ky}}{k} \right) \quad (12)$$

where x_0 , α , y , and k = parameters of Jenkinson's (1969) form of the GEV distribution. For $k = 0$, Equation 12 simplifies to asymptote I (often called the Gumbel or Fisher-Tippett Type I distribution):

$$x = x_0 + \alpha y \quad (13)$$

For asymptote II (often called a Frechet or Fisher-Tippett Type II distribution), k is negative; and for asymptote III (often called a Weibull or Fisher-Tippett Type III distribution), k is positive. Figure 8 gives a schematic representation of the three asymptotes in this context.

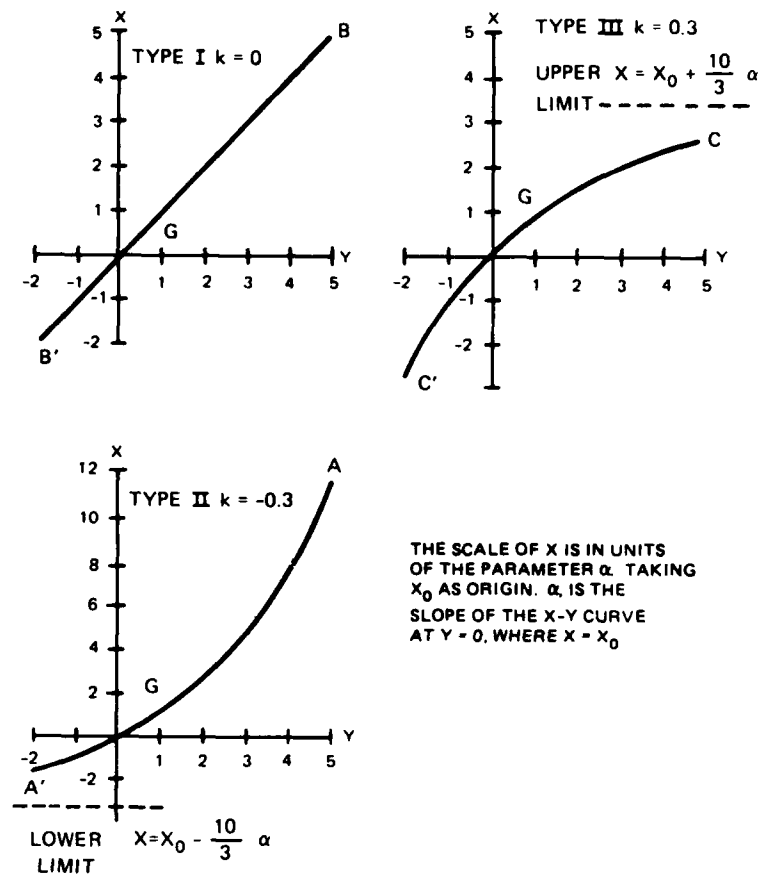


Figure 8. Schematic representation of the three Fisher-Tippett asymptotic distributions on X - Y diagrams (Jenkinson 1969)

16. Given values of x_0 , α , and k in Jenkinson's equation, a parametric relationship between the value x and return period is obtainable as

$$x = x_0 + \frac{\alpha}{k} - \frac{\alpha}{k} e^{-ky} \quad (14)$$

where y is given as a function of return period by

$$y = -\ln \left[\ln \left(\frac{T}{T-1} \right) \right] \quad (15)$$

for $y > 10$; this is close to $y = \ln(T - 1/2)$. For the case of $k = 0$, the equation for x simplifies to $x = x_0 + \alpha y$. In the context here, this equation linking x and T will be referred to as the GEV parametric equation.

17. In the context of the GEV parametric equation, it is apparent that, for the Fisher-Tippett Type III distribution, $x_0 + \alpha/k$ provides an explicit representation of the asymptotic upper bound for the distribution. In certain processes, this information can be very useful for design purposes.

18. It is important to note that the total methodology outlined in this section can provide a good objective estimate of expected extreme runups. Thus, to a certain extent, it gives a framework for research needs since it shows which functional relationships and statistical relationships must be evaluated before the entire problem can be regarded as reasonably solved.

New Data Sets

19. As part of this study, runup data from two new sites were analyzed. These data come from a field study in the San Francisco Bay area by Carlson (1984). Figure 9 shows the two sites involved in this study: Alameda Beach and Coyote Point. Details in the experimental setup can be found in Carlson (1984). Basically, data available for analysis consist of one incident wave height time series and corresponding runup time series at Alameda Beach and one incident time series of waves (sampled at four locations along a transect normal to shore) with four corresponding runup time series (taken from four different transects through the swash zone).

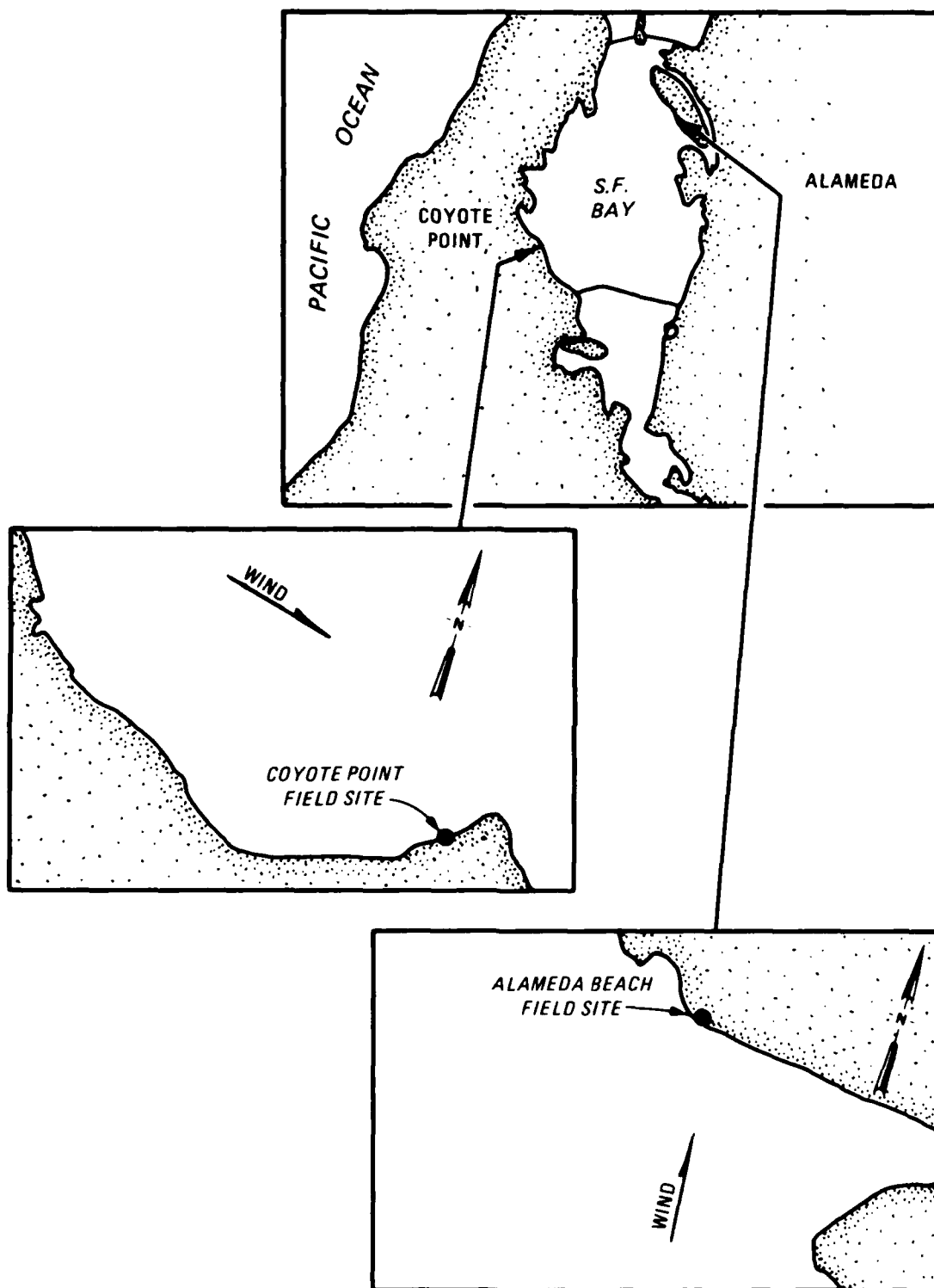


Figure 9. Maps showing locations of Alameda Beach and Coyote Point field sites (after Carlson 1984)

20. In Carlson's experiments waves are most likely locally generated since no oceanic swell can arrive at these sites. Since wind speeds in the experiments are relatively low, incident waves, wave periods, and runups are considerably smaller than those observed at the FRF site. Consequently, analysis of these data should provide a good check on general scaling relationships evident in Figures 1-7.

Analysis of Available Data

Analysis of R_2 and \hat{R}_2

21. Analysis of runup extremes from Carlson's experiments began by determining individual runups by an upcrossing method. For each time series, the largest 15 runups, defined as an excursion distance from trough to crest H_R and also as the maximum distance traveled up the beach R , were measured. In the context used here all variables are measured around the mean water level, rather than from some fixed datum.

22. Incident wave height parameters and beach slopes are taken directly from Carlson (1984) and are listed along with estimates of R_2 , \hat{R}_2 , and ξ in Table 2. As was seen in the earlier analysis of Holman runup data relative to wave measurements from different offshore locations, possibly the worst predictions of runup are given by waves inside the surf zone. Carlson, in his discussion of incident wave conditions at Coyote Point, indicated that the two innermost gages in his experiment were in a region where a substantial number of waves were breaking by plunging; therefore, the outermost gage will be used here to characterize incident wave conditions. Given its proximity to the surf zone, this outermost gage is likely to be reasonably consistent with wave conditions measured at gage 625 in the experiment at the FRF site.

23. Figure 10 shows data taken from the Carlson experiments plotted against the background of Figure 3. As can be seen there, data from these two additional sites appear to fit the same pattern as data from the FRF site. This suggests the scaling relationship between \hat{R}_2 and ξ is probably applicable to most natural (sand) beaches.

Analysis of $F(\hat{R})$

24. Although R_2 and \hat{R}_2 are useful parameters that provide a consistent measure of extreme runups, as was concluded earlier, a complete estimation methodology for extreme runup must involve the cumulative distribution

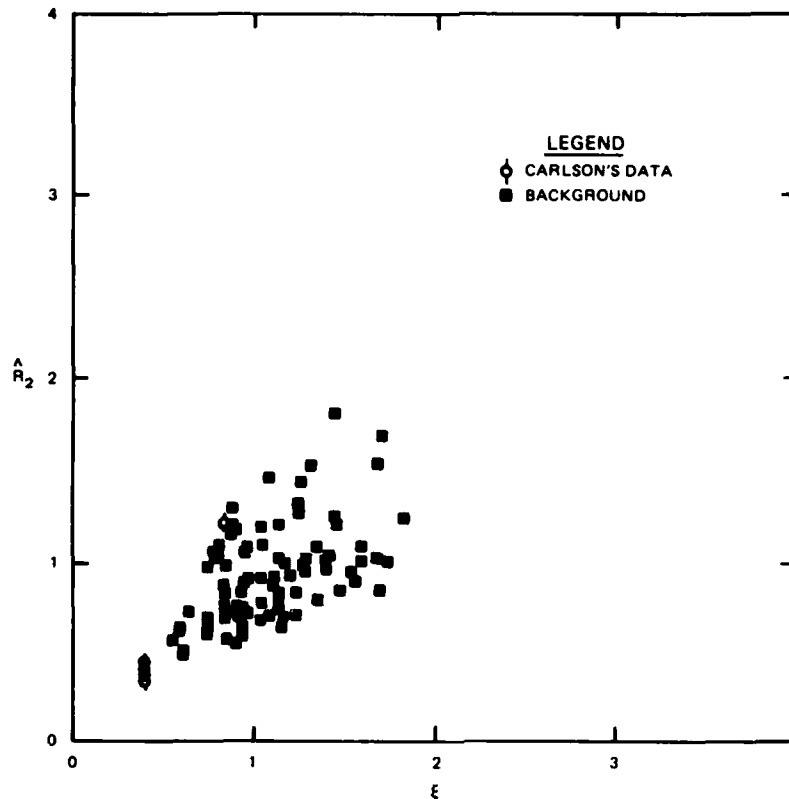


Figure 10. Data taken from the Carlson experiments plotted against the background of Figure 3, page 625

function of runups $F(\hat{R})$. This section shall attempt to derive a functional relationship between R and $F(R)$, based on selected data from Holman (1986) and Carlson (1984).

25. In order to obtain a consistent measure for $F(\hat{R})$ in the tail of the population, a subsample of 32 time series from the Holman data was selected and the 15 largest runups in each series were determined. Using the plotting position due to Gumbel, estimates for $F(\hat{R})$ can be given for each runup series by

$$F(\hat{R}) = 1 - \frac{i}{m+1} \quad (16)$$

where

i = rank of the runup value (largest = 1, second largest = 2, etc.)

m = total number of runups, determined from an upcrossing method

Since a functional relationship between \hat{R} and ξ is expected to exist, a more consistent form for the cumulative distribution function should be obtained in terms of a new parameter \hat{R}' given by

$$\hat{R}' = \frac{\hat{R}}{\xi} \quad (17)$$

where ξ is defined in terms of the local wavelength.

26. Since we are primarily interested in extremes, let us define non-counter probability for given runups as

$$N(\hat{R}') = 1 - F(\hat{R}') \quad (18)$$

Figure 11 shows a plot of $\log_{10} N(\hat{R}')$ versus \hat{R}' , which indicates that indeed the behavior of $N(\hat{R}')$ is quite structured for the 32 selected data points. In this figure the base 10 logarithm is used to provide a better display of behavior of the extremes. Two heavy lines in addition to the samples

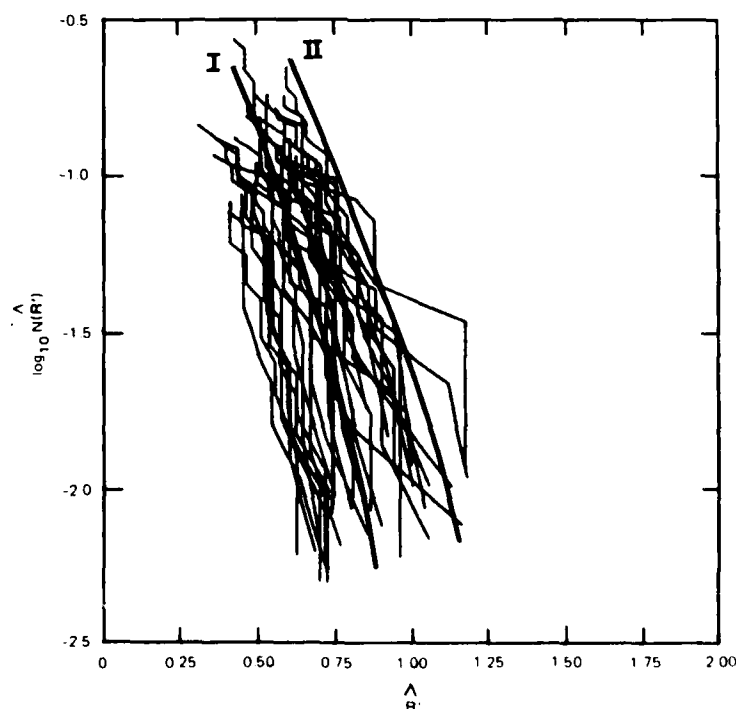


Figure 11. Sample of 15 largest runups for 32 selected cases from Holman

are shown in Figure 11. The first (marked I) represents an estimate of the mean of all data, and the second (marked II) represents a data envelope. Returning to the GEV equation, the two lines were found to be well represented by Equation 14, with the only significant difference being in the value of x_0 . This difference in x_0 represents a simple additive shift between envelope and mean value. Based on both analyses, the values of α and k for both curves are 0.20 and 0.19, respectively. The value for x_0 in curve I was found to be 0.20; whereas for curve II, x_0 was estimated to be 0.47.

27. Returning to Equation 12, the equation for the expected extremal estimation for a given runup can be written as

$$\hat{R}' = 0.20 + 0.20 \left[\frac{1 - \exp(-0.19y)}{0.19} \right] \quad (19)$$

where y is given in terms of Equation 14. In the context here, the recurrence interval T is given in terms of numbers of waves. Using the definition of T as

$$T = \frac{1}{1 - F(x)} = \frac{1}{N(x)} \quad (20)$$

any value of $N(x)$ can be substituted to obtain a corresponding value of \hat{R}' . Figure 12 gives a graphical example of the curves for the mean and envelope extrapolated out to values of $N(x) = 1/10,000$. For a 10-sec wave period, this would correspond to a duration of over 24 hr, which should provide a sufficient range for selection of a design value.

28. Once a design value for $N(x)$ is selected, Equation 17 or Figure 12 can be used to obtain actual dimensional estimates of expected runups. For example, for a 3-hr interval of high waves with a mean period of 10 sec, the expected largest wave would have a value of $N(x)$ of approximately $1/1,000$. From Figure 12, it can be seen that \hat{R}' is therefore equal to 0.976. This can be converted into a dimensional estimate by recalling the definition of \hat{R}' . Thus, this case would have

$$R = 0.976\beta(HL)^{1/2} \quad (21)$$

29. For the Carlson data, a similar analysis to that described above

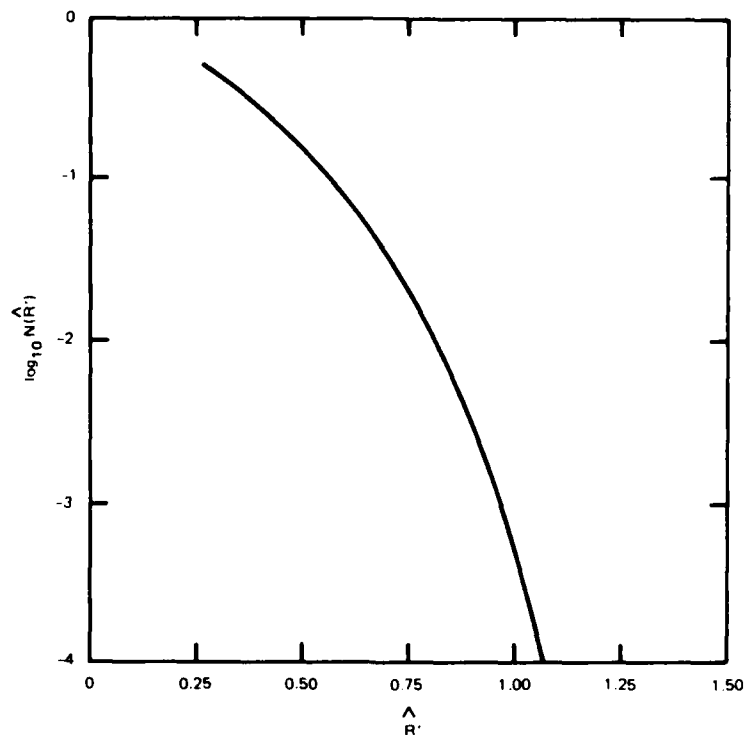


Figure 12. Plot of extremal distribution for expected runups

was also completed. Figure 13 shows a plot of Alameda Beach data, and Figure 14 shows a plot of Coyote Point data. As can be seen in a comparison between these plots and Figure 11, once again the behavior of runup on these beaches follows the same general pattern as that observed at the FRF site. Estimation of x_0 , α , and k parameters for the GEV analysis indicates parameter values for the FRF data set can also give a reasonable approximation to the estimates of $F(\hat{R}')$ from Carlson's runup data at Coyote Point. However, the data from Alameda appear somewhat inconsistent with the rest of the runup data. It is possible that the stake at which incident waves were measured for Alameda was inside the breaker zone, and therefore the wave data are spurious in a manner similar to that of gage 615 at the FRF site in terms of their relation to runup. For wave data outside of the immediate surf zone, the equations for $F(\hat{R}')$ can probably be regarded as a good first approximation to the actual cumulative distribution function.

Conclusions and Recommendations

30. This report had three primary objectives as noted in the

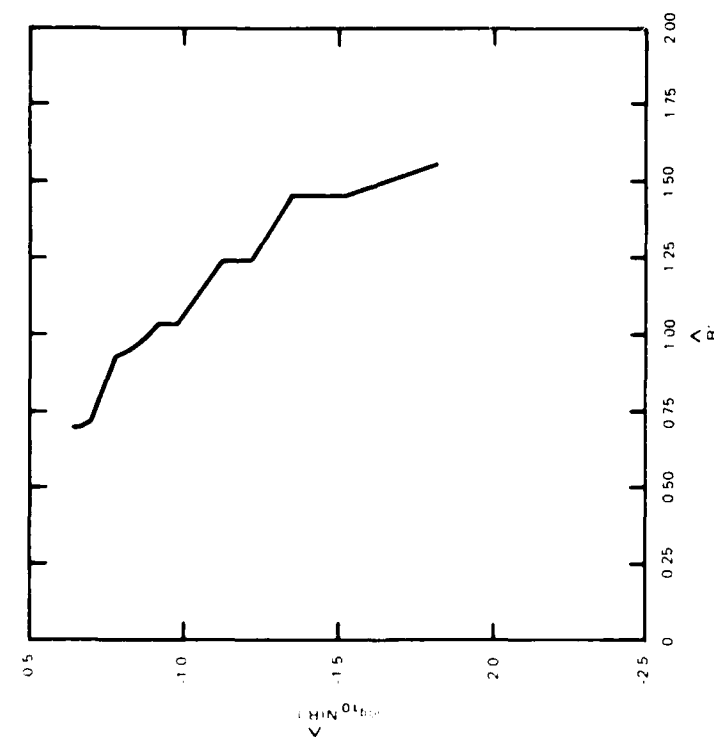


Figure 13. Plot of Alameda Beach data from analysis of the Carlson data

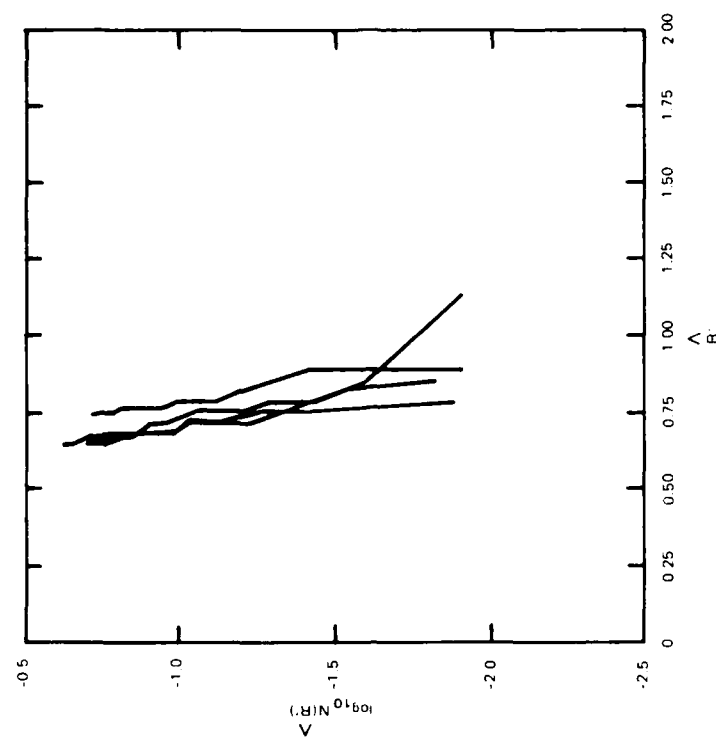


Figure 14. Plot of Coyote Point data from analysis of the Carlson data

Introduction. The first of these was to supplement the extensive runup data set for natural beaches taken at CERC's FRF. Secondly, a review of available data sets was to be made in order to examine consistency, in terms of runup prediction, of wave measurements from different depths. Finally, a statistical framework for estimating extreme runups during storms was to be formulated.

31. Relative to the first objective, data from runup measurements at two beaches in the San Francisco Bay were analyzed in a manner consistent with the FRF data set. Data from these additional sites fit quite well into the same empirical framework as the FRF data. These results suggest that relationships between wave and runup parameters based on the FRF data are also valid for other natural beaches.

32. In order to examine consistency of wave data from different depths relative to predictability of runup, FRF runup data were plotted against surf similarity parameters based on incident wave conditions measured at gages 620, 625, and 615, located in mean depths of about 17, 8, and 2 m, respectively. These plots showed the best predictor of runup was available using data from gage 625 scaled by local wavelength, rather than deep-water wavelength. Results for gage 615 showed a large amount of erratic scatter, which suggests that measurements too close to shore (littoral environmental observations) are not particularly good predictors of runup. Results for gage 620 were relatively well organized, but contained some outliers which were not apparent in the results for gage 625. This suggests that wave measurements should be taken at a consistent depth for future runup experiments. Additional analyses should be aimed at contributing toward a better understanding of the physics of wave transformations and runup in order to increase the ability to predict runup from arbitrary wave data sets.

33. Finally, it has been shown that factors contributing to prediction of wave runup can be incorporated into a coherent statistical framework. Within this framework, the cumulative distribution function and nonexceedance probability play major roles in estimating expected extreme runups over a fixed interval with constant incident wave and water-level conditions or over an entire storm with variable wave conditions and water levels. As shown in Figure 12, the estimation procedure for idealized, constant conditions can be simplified to a graphical method.

References

- Borgman, L. E. 1973. "Probabilities for Highest Wave in Hurricane," Journal of Waterway, Port, Coastal and Ocean Engineering, American Society of Civil Engineers, Vol 99, No. WW2, pp 187-207.
- Bouws, E., et al. 1985. "Similarity of the Wind Wave Spectrum in Finite Depth Water; Part I. Spectral Form," Journal of Physical Oceanography.
- Carlson, C. T. 1984. "Field Studies of Run-up Generated by Wind Waves on Dissipative Beaches," prepared under SRI IR&D Project 634D32-BUA, SRI International, Menlo Park, Calif.
- Fisher, R. A., and Tippett, L. H. C. 1928. "Limiting Forms of the Frequency Distribution of the Largest or Smallest Member of a Sample," Proceedings, Cambridge Philosophical Society, Vol 24.
- Holman, R. A. 1986. "Extreme Value Statistics for Wave Run-up on a Natural Beach," Coastal Engineering, Vol 9, pp 527-544.
- Jenkinson, A. F. 1955. "The Frequency Distribution of the Annual Maximum (or Minimum) Values of Meteorological Elements," Quarterly Journal, Royal Meteorological Society, Vol 81, pp 158-171.
- _____. 1969. "Statistics of Extremes," Estimation of Maximum Floods, Technical Note 98 (WMO-No. 223, Pt. 126), Chapter 5, World Meteorological Organization, Geneva, Switzerland, pp 183-227.
- Resio, D. T. 1986a. "Shallow-water Waves -- Part I: Theory," Journal of Waterway, Port, Coastal, and Ocean Engineering, American Society of Civil Engineers, accepted for publication.
- _____. 1986b. "Shallow-water Waves -- Part II: Data Comparisons," Journal of Waterway, Port, Coastal, and Ocean Engineering, American Society of Civil Engineers, accepted for publication.

Table 1
Wave Heights and Periods for Two Selected Time Intervals
Covered by Holman's Data

Date*	Gage 620		Gage 625	
	Wave Height m	Wave Period sec	Wave Height m	Wave Period sec
82101214	2.36	16.20	3.11	16.34
82101214	2.36	16.20	3.11	16.34
82101214	2.36	16.20	3.11	16.34
82101214	2.36	16.20	3.11	16.34
82101215	2.26	15.10	3.12	16.52
82101215	2.26	15.10	3.12	16.52
82101215	2.26	15.10	3.12	16.52
82101217	2.39	16.50	3.13	16.61
82101217	2.39	16.50	3.13	16.61
82101217	2.39	16.50	3.13	16.61
82101217	2.39	16.50	3.13	16.61
82101218	2.45	16.30	3.13	16.70
82101218	2.45	16.30	3.13	16.70
82101218	2.45	16.30	3.13	16.70

82102413	3.51	8.10	3.44	8.90
82102413	3.51	8.10	3.44	8.90
82102415	3.75	9.60	3.37	9.52
82102509	4.05	13.80	3.33	13.53
82102509	4.05	13.80	3.33	13.53
82102512	3.65	13.30	3.19	13.35
82102512	3.65	13.30	3.19	13.35

* This column is read: year, month, day, hour (on a 24-hr clock).

Table 2
Runup Parameters for Alameda Beach
and Coyote Point Experiments*

<u>Location</u>	<u>H_s</u>	<u>T_m</u>	<u>Tan β</u>	<u>R₂</u>	<u>[^]R₂</u>	<u>ξ</u>
Alameda Beach	0.14	2.4	0.11	0.165	1.17	0.88
Coyote Point #3	0.28	2.4	0.08	0.091	0.33	0.45
Coyote Point #4	0.28	2.4	0.08	0.092	0.34	0.45
Coyote Point #5	0.28	2.4	0.08	0.104	0.37	0.45
Coyote Point #6	0.28	2.4	0.08	0.103	0.36	0.45

-
- * H_s = Significant wave height, in metres
 T_m = Wave period of spectral peak, in seconds
 tan β = Beach slope
 R₂ = 2-percent runup, in metres
 [^]R₂ = Normalized 2-percent runup
 ξ = Iribarren parameter

END

8-87

DTIC